



## Features of the formation process of steel coatings by supersonic metallization

Serik Nurakov<sup>1</sup>, Marat Belotserkovsky<sup>2</sup>, Assel Tulebekova<sup>3</sup>, Merkhata Shugayev<sup>4</sup>

<sup>1</sup>National University of Defense of the First President of the Republic of Kazakhstan - Elbasy, Nur-Sultan, Kazakhstan, serik.nurakov@inbox.ru

<sup>2</sup>L.N.Gumilyov Eurasian National University, Nur-Sultan, Kazakhstan, gulnara.merzadinova@mail.ru

<sup>3</sup>L.N.Gumilyov Eurasian National University, Nur-Sultan, Kazakhstan, gulnara.merzadinova@mail.ru

<sup>4</sup>National University of Defense of the First President of the Republic of Kazakhstan - Elbasy, Nur-Sultan, Kazakhstan, merkhata.shugayev@inbox.ru

### ABSTRACT

The formation process of steel coatings by the supersonic method using the AAM-10 apparatus and an experimental sample of a metallizer with an adjustable electrode position was studied. It was found that the main parameters that determine the quality of the coating are the temperature and pressure of the gas in the spray head. The effect of these parameters on the size of dispersible particles, as well as their velocity in the jet and the effect of the flow of atomizing gas on the amount of oxygen in the coatings, was experimentally established. The density and adhesion of the coatings were obtained depending on the spraying distance and air flow. The influence of current strength on the quality of coatings is established. Rational spraying regimes are obtained.

**Key words :** supersonic speeds, atomizing gas, temperature, pressure, flow, porosity, performance.

### 1. INTRODUCTION

The most effective and economical today is the technology of supersonic (hypersonic) metallization (SM) [1,2,3,4], which differs from traditional electrometallization (EAM) by using a continuous energy source to heat a gas atomizing particles melted in an electric arc of a wire. In the process of metallization, the spraying of liquid metal formed as a result of the thermal effect of an electric arc on the ends of two wire electrodes is performed by a stream of combustion products of a propane-air mixture.

In this case, the jet velocity at the exit from the nozzle reaches 1500 m / s at a temperature of 2200 K, and the high-velocity flow head is  $23.5 \cdot 10^4 \text{ kg / m} \cdot \text{s}^2$ , which is three times more than with plasma spraying. This allows the molten metal particles to move faster than 500 m / s and form a coating that has increased adhesion to the substrate than with EAM. This

method forms coatings taking into account porosity from 3% for non-ferrous metals and up to 7% for steel composite wires. The adhesion tensile strength of the sprayed layers is more than 45 MPa.

For applying coatings, we used the installation of the AAM-10 model of the Academy of Sciences of the Republic of Belarus [5,6,7] and the design of the apparatus according to the patent of the Republic of Kazakhstan for a utility model [8,9], the sprayed materials were wires made of steel 95X18Sh, 40X13 and 12X18H10T. To increase the adhesion strength of the coatings to the base, an intermediate layer was applied by spraying a wire of X20H80 alloy.

As the material of the samples used low-carbon steel Art. 3. Before applying the coating, blasting and abrasive treatment was carried out at a working pressure of compressed air of 0.6 MPa and a consumption of steel chipped fractions of the FSC 0.3-2.0 grade of about 1.2 kg / s. To determine the flight speed of particles of the sprayed material, a speed meter of luminous objects of the ISSO-1 type was used. By changing the speed of rotation of the mirror in the device, we achieved the parallelism of the tracks of luminous particles and the control lines visible in the eyepiece of the device, after which the speed value was calculated using the arrow indicator. To measure the speed of particles in different areas of the spray cone, a copper water-cooled screen was used, through the longitudinal slit of which the speed of particles was recorded with ISSO-1. This method made it possible to quickly determine the maximum  $v_{\text{max}}$  and minimum  $v_{\text{min}}$  particle velocities.

### 2. MATERIALS AND METHODS

The phase composition was studied using a DRON-3 diffractometer (monochromatized ( $\text{C}_0\text{K}_\alpha$ ) radiation). The diffraction lines were recorded in the following mode: scanning step —  $0.1^\circ$ , the pulse acquisition time at the point — 10 sec.

The porosity of the coatings was evaluated on metallographic sections using the Autoscan software package for image processing and analysis. Vickers microhardness was

measured on a DuraScan 20 hardness tester with a load on 0.24N indenter.

### 3. RESULTS AND DISCUSSION

It is known that the temperature of the electric arc between wire electrodes significantly accelerates the physical and chemical processes: burnout of impurities, dissociation of oxygen and nitrogen molecules into an atomic state, their interaction with metal, acceleration of crystallization, cracking and, thereby, significantly determines the quality of the metal coating .

It has been theoretically established that an increase in the initial temperature of the atomizing gas (Figure 1) increases the coefficient of aerodynamic force acting on a particle of molten metal. Moreover, with decreasing particle diameter, the efficiency of increasing the temperature of the jet increases sharply. An increase in the pressure of the atomizing gas leads to a decrease in the drag coefficient  $C_x$ , which is explained by an increase in the degree of cooling of the gas when it expands in the Laval nozzle with a corresponding decrease in the kinematic coefficient of viscosity of the flow. Most significantly,  $C_x$  decreases with an increase in the initial pressure  $P_0$  to 0.6–0.8 MPa, then it remains almost unchanged to 2.5 MPa. An increase in pressure in the spray head leads to an increase in the aerodynamic force of the jet, but at  $P_0 > 0.6$  MPa the efficiency of increasing the pressure before the critical section of the nozzle decreases.

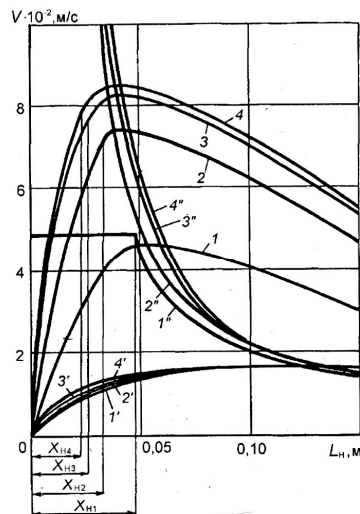


**Figure 1:** The influence of atomizing gas temperature (1, 1', 1''- 290 K; 2, 2', 2''- 1500 K; 3, 3', 3''- 3000 K; 4, 4', 4''- 5000 K) on changing particle velocities with size (1, 2, 3, 4-5  $\mu\text{m}$ ; 1', 2', 3', 4'- 100  $\mu\text{m}$  and jet 1'', 2'', 3'', 4'') along the axis at  $P_0 = 0.6$  MPa;  $R_a = 3$  mm.

It should be noted that in addition to the main parameters of the spraying gas  $T_0$  and  $P_0$ , the geometric parameters of the metallizer spraying system, such as the radius of the nozzle at the cut and the distance from the melting center of the wire electrodes to the cut of the nozzle  $X_1$ , have a significant effect

on the maximum particle velocity. An increase in the radius of the nozzle  $R_a$  increases the maximum velocity of the particles by lengthening their acceleration section (Figure 2).

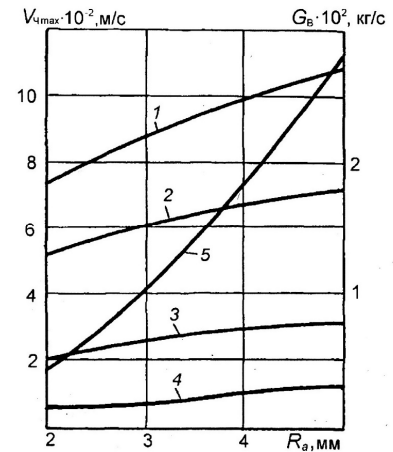


**Figure 2:** The dependence of the maximum particle velocity of size: 1-5  $\mu\text{m}$ ; 2-10  $\mu\text{m}$ ; 3-40  $\mu\text{m}$ ; 4-200  $\mu\text{m}$  and spray gas flow (5) from the radius of the nozzle at  $T_0 = 3000$  K and  $P_0 = 1.0$  MPa

Experimental studies of the effect of the degree of heating of the spraying gas on the average particle size of the dispersible metal showed that with a decrease in  $T_0$  to 2300-2500 K, it decreases, reaching 10-15  $\mu\text{m}$  (the size range of each fraction was assumed to be 5  $\mu\text{m}$ ). A further increase in  $T_0$  leads to an increase in the fraction of particles of fine fractions, however, the fraction of 10–15  $\mu\text{m}$  remains at its maximum all the time, determining the average particle size. The analysis showed that it is advisable to limit the heating temperature of the spraying gas to 2300-2500 K, since its further increase does not significantly affect the average size, weight average velocities, and particle temperature. Experimental studies of the effect of the degree of heating of the spraying gas on the average particle size of the dispersible metal showed that with a decrease in  $T_0$  to 2300-2500 K, it decreases, reaching 10-15  $\mu\text{m}$  (the size range of each fraction was assumed to be 5  $\mu\text{m}$ ). A further increase in  $T_0$  leads to an increase in the fraction of particles of fine fractions, however, the fraction of 10–15  $\mu\text{m}$  remains at its maximum all the time, determining the average particle size. The analysis showed that it is advisable to limit the heating temperature of the spraying gas to 2300-2500 K, since its further increase does not significantly affect the average size, weight average velocities, and particle temperature.

Thus, it was found that the supersonic process of electric arc metallization by heating the spraying gas allows to increase the flight speed of particles smaller than 40  $\mu\text{m}$ , practically without affecting the speed of larger particles. In this case, with a decrease in particle size, the degree of increase in their velocity increases with increasing temperature of the atomizing gas. For particles with a diameter of less than 40  $\mu\text{m}$ , the main increase in speed (80-90% of the maximum) occurs in the initial section of the jet, the length of which for the studied range of temperature (up to 5000 K) and pressure

(up to 2.5 MPa) spraying air is 25-50 mm (with a nozzle diameter at a cut of 6 mm). The maximum flight speeds of such particles are achieved at distances of 40-60 mm from the melting center of the wire electrodes.

It is advisable to limit the temperature of the preliminary heating of the spray gas to 2300-2500 K, and the pressure to 0.6-0.8 MPa, since a further increase in these parameters does not significantly affect the average speed, size, and temperature of the particles.

The composition of the spraying propane-air torch of the supersonic metallization apparatus was chosen as follows: mode 1 — excess propane with a volume ratio of air and propane  $\beta=17-20$  mode 2 — excess air  $\beta=26-28$  mode 3 — clean air (traditional electric arc metallization scheme).

Since the main amount of oxides is formed as a result of the contact of molten particles with air, the effect of spray air flow on the amount of oxygen in coatings obtained by traditional metallization was studied (mode 3). It was found that the oxygen content in electrometallization coatings is 2.6-4.2% depending on the flow of compressed air, and the maximum concentration of 4.2% is achieved at a flow rate of about 1.4-1.6 m<sup>3</sup> / min (Figure 3). A further increase in spray air flow does not lead to a noticeable increase in oxygen concentration.

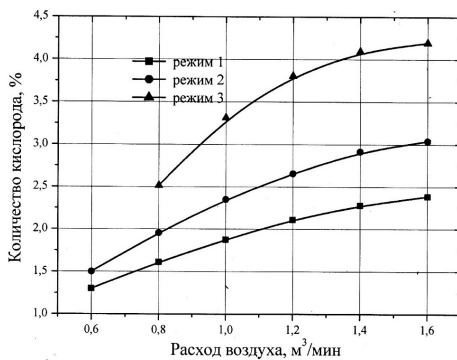


**Figure 3:** The effect of the flow rate of spraying air in the jet on the amount oxygen in coatings obtained under various conditions

The smallest amount of oxygen (1.3-2.3%) is recorded in coatings sprayed with an excess amount of propane in the mixture (mode 1). The increase in air in the combustible mixture to an almost limit value ( $\beta=28$ ) increases the oxygen content, however, the degree of oxidation of the coatings remains lower than with traditional metallization.

The study of the density and adhesion of the sprayed coatings showed that the porosity increases sharply, and the adhesion strength decreases with an increase in the spraying distance over 200  $\mu\text{m}$  (Figures 4.5). This is especially evident when the minimum allowable flow rates of compressed air are 1-1.5 m<sup>3</sup> / min., And with an increase in air flow rates to maximum values, the porosity decreases monotonically. The minimum flow rate is determined by the stability of combustion of the combustible mixture, the maximum is determined by the flow rate of combustible gas (propane) from the cylinder.

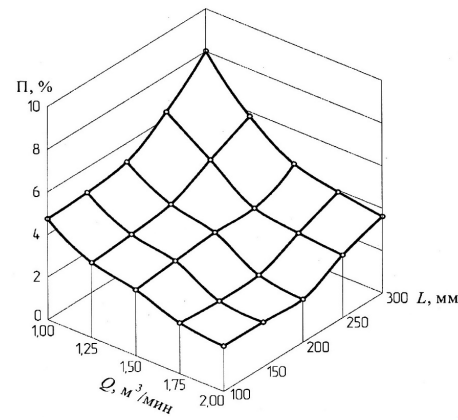


**Figure 4:** Dependence of the porosity of steel coatings on flow air (Q) and spraying distances (L)

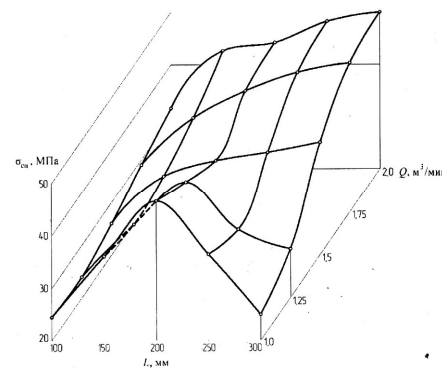


**Figure 5:** Effect of air flow and spraying distance on the adhesion strength of steel coatings to the base

A further increase in consumption will ensure an increase in the quality of the coating, however, this will require complication of the technological scheme of the process to ensure the necessary consumption of propane, for example, propane supply from the ramp. In most cases, such a rise in price of the process is impractical.

With an increase in the spraying distance over 200 mm, the speed and heat content of the droplets decrease. When impacted for this reason, the conditions for the spreading of the liquid metal drop over the surface are worsened. This leads to an increase in the porosity of the coating. Small distances,  $L = 100-150$  mm, it is technologically difficult to provide in corners and on surface ledges.

Thus, the studies showed that the most dense coatings with an acceptable amount of oxides during hypersonic metallization of alloyed steels are formed when using a propane-air mixture with an excess of propane  $\beta=18-20$ , air consumption in the mixture  $Q = 1.75-2$  m<sup>3</sup> / min, spraying distance  $L = 150-170$  mm.

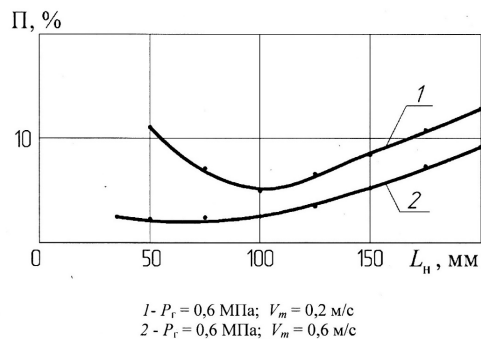


**Figure 6:** Dependence of the porosity of steel coatings on spraying distance

Figure 6 shows the dependences of the porosity of the coatings obtained by the supersonic metallization method on the spraying distance at various speeds of the metallizer relative to the sprayed surface. The porosity of the coatings obtained at a minimum velocity of the metallizer, i.e. when coating in one pass, while reducing the spraying distance, it first decreases and then grows up to the values characteristic of coatings obtained by the traditional electrometallization method.

An increase in the speed of movement of the metallizer leads to a noticeable decrease in the porosity of the coatings obtained by supersonic metallization at short distances  $L_{н} = 80-100$  mm.

In the process of determining the rational electrical parameters of the process, it was found that the magnitude of the operating current at a voltage of 26-30 V is directly proportional to the productivity of the deposition process of steel coatings (table 1).

**Table 1:** The influence of the operating current of the arc on the performance of the process of spraying steel wires

Amperage, A	Spraying capacity (kg / h) of steel wires of various diameters	
	1,6 mm	2.0 mm
60	1,5	1,5
100	3.00	4,5
150	4.00	6,5
200	5.00	8,0
250	6.00	10,0
300	7.00	14,0
350	8.00	15,0
400	9.00	16,0
450	10.00	18,0

The research results obtained during the application of steel coatings by traditional electric arc metallization show [12] that the voltage in the arc of the metallizer must be set depending on the requirements for the coating. If the steel wear-resistant coating works at specific loads not exceeding 10 MPa, then spraying should be carried out at the lowest possible voltage. In this case, the utilization of metal during spraying will be the highest. When forming steel coatings operating under severe conditions, it is recommended to apply

the application at increased voltage to increase adhesion. The experiments showed that this is also true for the process of supersonic metallization.

The study of the influence of the operating arc current on the porosity of the coatings showed (Table 2) that, at high values of the arc current (250-450 A), increasing the speed of the  $V_{TİM}$  metallizer relative to the restored part significantly reduces the layer porosity, and when spraying at low current (60-100 A)  $V_{TİM}$  practically does not affect this value.

**Table 2:** The influence of arc amperage on the porosity of coatings

Amperage A	The porosity of the coatings (%) at different speeds of the metallizer (m / s)		
	0,04	0,2	0,6
60	1,8	1,5	1,3
100	2,0	1,7	1,4
150	2,7	1,8	1,4
200	3,0	2,1	1,5
250	3,5	2,3	1,6
300	4,1	2,6	1,6
350	4,5	2,9	1,7
400	5,2	3,3	1,8
450	5,6	3,5	1,8

### 5. CONCLUSION

An analysis of the experimental results allowed us to determine the following rational modes of deposition of steel coatings on parts of the “shaft” type by the method of supersonic metallization:

- for shafts with a diameter of 60 to 100 mm and a spray wire diameter of 1.6 mm, arc voltage 26 V, arc current 350 A, part speed 65-70 rpm .;
- for the diameter of the sprayed wires 2 mm - arc voltage 30 V, arc current 250 A, part speed 70-75 rpm .;
- for shafts with a diameter of 100 to 200 mm and a diameter of spray wires of 1.6 mm - arc voltage 28-30V, arc current 350 A, part speed 75-90 rpm .;
- for the diameter of the sprayed wires 2 mm - arc voltage 30-32 V, arc current 350 A, part rotation speed 90-110 rpm .;
- for shafts with a diameter of 200 to 300 mm and a spray wire diameter of 1.6 mm - arc voltage 30-32 V, arc current 350 A, part rotation speed 90-110 rpm .;
- for the diameter of the sprayed wires 2 mm - arc voltage 34 V, arc current 350 A, part speed 110-120 rpm.

Thus, it is shown that the heating temperature of the spraying gas in the combustion chamber of the gas turbine unit should be limited to 2300-2500 K, and the pressure to 0.6 ... 0.8 MPa. It was found that the amount of oxygen is 1.5-2.0 times less than with the traditional electrometallization method.

The electrical parameters of the gas turbine unit process and the speed of the metallizer are determined, which provide high-quality coatings when spraying alloy steel wires.

The most dense coatings with an acceptable amount of oxides in the process of gas turbine unit alloy steels are formed when using a propane-air mixture with an excess of propane ( $\beta=18-20$ ), air consumption in the mixture  $Q = 1.75-2m3 /$

min., Spraying distance  $L = 150-170$  mm. Moreover, the quality of such coatings is commensurate with the results obtained by the authors during chemical-thermal and microplasma treatment.

## ACKNOWLEDGEMENT

This article is published as part of the research work of program-targeted funding № BR 05236855 "Military-technical and military-technological support of the defense and security of the Republic of Kazakhstan on the basis of economic pragmatism".

## REFERENCES

1. Barkhordari A and Ganjovi A. **Technical characteristics of a DC plasma jet with Ar/N<sub>2</sub> and O<sub>2</sub>/N<sub>2</sub> gaseous mixtures**. Chin. J. Phys., 2019, 57, 465–78.
2. Belotserkovsky M. A. **Improvement of equipment and technologies of high-speed electric arc metallization**. Strengthening technologies and coatings, 2017, 13 (11), 500-506.
3. Bora B, Aomoa N and Kakati M. **Characteristics and temperature measurement of a non-transferred cascaded dc plasma torch**. Plasma Sci. Technol., 2010, 12, 181–7.
4. Busby K, Corrigan J, Yu S T, Hoke J, Cathey M and Gundersen M. Effects of corona, spark and surface discharges on ignition delay and deflagration-to detonation times in pulsed detonation engines 45th AIAA Aerospace Sciences Meeting and Exhibit (Nevada: Reno) (<https://doi.org/10.2514/6.2007-1028>).
5. Sydyknazarov, M.-A., Karzhaubay, J., Sydyknazarova, S., Bayurzhan, M. **Values of the youth of Kazakhstan**. New Educational Review, 2018, 52(2), c. 137-148.
6. Li, B.; Zhu, Y.; Wang, Z.; Li, C.; Peng, Z.R.; Ge, L. **Use of multi-rotor unmanned aerial vehicles for radioactive source search**. Remote Sens. 2018, 10, 728.
7. Royo, P.; Perez-Batlle, M.; Cuadrado, R.; Pastor, E. Enabling dynamic parametric scans for unmanned aircraft system remote sensing missions. J. Aircr. 2014, 51, 870–882.
8. mRo Pixhawk Flight Controller (Pixhawk 1). Available online: [https://docs.px4.io/en/flight\\_controller/mro\\_pixhawk.html](https://docs.px4.io/en/flight_controller/mro_pixhawk.html) (accessed on 10 September 2018).
9. Meier, L.; Tanskanen, P.; Heng, L.; Lee, G.H.; Fraundorfer, F.; Pollefeys, M. **PIXHAWK: A Micro Aerial Vehicle Design for Autonomous Flight Using Onboard Computer Vision**. Auton. Robots 2012, 33, 21–39. [CrossRef]
10. PX4 Flight Stack. Available online: <http://px4.io/> (accessed on 10 September 2018).
11. Ardupilot Flight Stack. Available online: <http://ardupilot.org/copter/> (accessed on 10 September 2018).
12. SF11/C (120 m) Lightware Laser Altimeter. Available online: <https://lightware.co.za/products/sf11-c-120-m> (accessed on 10 September 2018).
13. Mission Planner Overview. Available online: <http://ardupilot.org/planner/docs/mission-planner-overview.html> (accessed on 10 September 2018).
14. Aubakirova, G., Adilbekov, Z., Narbayev, S. **Influence of water mineralization on zooplankton productivity in reservoirs of Akmola region**. Periodico Tche Quimica, 2020, 17(34), c. 520-527
15. Raspberry Pi 3 Model B+. Available online: <https://www.raspberrypi.org/products/raspberry-pi-3-model-b-plus/> (accessed on 10 September 2018).
16. RITEC Radiation Micro Spectrometer uSPEC. Available online: <http://www.ritec.lv/uspec.html> (accessed on 10 September 2018).
17. DJI F550 ARF. Available online: <https://www.dji.com/es/flame-wheel-arf> (accessed on 11 September 2018).
18. Gilmore, G. Practical Gamma-Ray Spectroscopy; John Wiley & Sons Ltd.: West Sussex, UK, 2008.
19. International Atomic Energy Agency (IAEA). **Safety of Radiation Sources: International Basic Safety Standards, General Safety Requirements**, IAEA Safety Standards Series No. GSR Part 3; IAEA Publications: Vienna, Austria, 2014.
20. Aubakirova, G.A., Pishenko, Y.V., Maikanov, B.S. **Comprehensive study of the Ashykol and Kumkol lakes of Akmola Oblast of the North Kazakhstan**. Mediterranean Journal of Social Sciences, 2014, 5(23), c. 2607-2611
21. Aubakirova, G.A., Syzdykov, K.N., Kurzhykayev, Z., Sabdinova, D.K., Akhmedinov, S.N. **Quantitative development and distribution of zooplankton in medium lakes of the Kostanay Region (North Kazakhstan Region)**. International Journal of Environmental and Science Education, 2016, 11(15), c. 8193-8210, ijese.2016.620
22. Somzhurek, B.Z., Yessengaliyeva, A.M., Medeubayeva, Z.M., Makangali, B.K. **Central Asia and regional security. Communist and Post-Communist Studies**, 2018, 51(2), c. 161-171.
23. Sempau, J.; Badal, A.; Brualla, L. A PENELOPE-based system for the automated Monte Carlo simulation of clinacs and voxelized geometries—Application to far-from-axis fields. Med. Phys. 2011, 38, 5887–5895.
24. Gasull, M.; Royo, P.; Cuadrado, R. **Design a RPAS Software Architecture over DDS**. Master's Thesis, Castelldefels School of Telecommunications and Aerospace Engineering, Castelldefels, Spain, 2016.
25. Garro Fernandez, J.M. **Drone Configuration for Seaside Rescue Missions**. Master's Thesis, Universitat Politècnica de Catalunya, Barcelona, Spain, 2017.
26. Makangali, B., Amirbekova, S., Khamitova, M., Baydarov, E. **Religious aspects of the Syrian crisis on social media**. Central Asia and the Caucasus, 2020, 21(1), c. 102-111.
27. Macias, M. **Study of 4G Propagation Conditions Using Unmanned Aerial Systems**. Ph.D. Thesis, Universitat Politècnica de Catalunya, Barcelona, Spain, 2018.

28. **Cloud Cap Technology**. Piccolo II Product. 2017. Available online: <http://www.cloudcaptech.com/products/detail/piccolo-ii> (accessed on 7 July 2017).
29. Makangali, K. Konysbaeva, D.; Zhakupova, G.; Gorbulya, V.; Suyundikova, Zh. **Study of sea buckthorn seed powder effect on the production of cooked-smoked meat products from camel meat and beef**. Periodico Tche Quimica, 2019, 16: 130-139.
30. Lisitsyn A., Makangali K., Uzakov Y., Taeva A., Konysbaeva D., Gorbulya, V (2018) Study of the National Cooked Smoked Meat Products While Tests with Laboratory Animals at the Pathology Models with the Purpose to Confirm the set of Biocorrective Features. Current Research in Nutrition and Food Science journal 6(2): 536-551.
31. 38. Guava EventBus. Available online: <https://github.com/google/guava/wiki/EventBusExplained> (accessed on 12 September 2018).
32. 39. Message Queuing Telemetry Transport (MQTT). Available online: <http://mqtt.org/> (accessed on 12 September 2018).
33. 40. MAVLink Micro Air Vehicle Communication Protocol. Available online: <http://qgroundcontrol.org/mavlink/start> (accessed on 12 September 2018).
34. 41. Hibernate. Available online: <http://hibernate.org/> (accessed on 12 September 2018).
35. 42. H2 Database Engine. Available online: <http://www.h2database.com/html/main.html> (accessed on 12 September 2018).
36. 43. European Accreditation. EA-4/02 M: 2013 Evaluation of the Uncertainty of Measurement in Calibration. 2013. p. 75.
37. Dulambaeva, R., Orazalin, R., Tulembayeva, A., Peruashev, A. **Assessing the development effect of governance**. Life Science Journal, 2014, 11(SPEC. ISSUE 4), c. 144-152
38. Tulembayeva, A., Togusov, A., Berdibekov, A., Zhakashev, A. **Assessment of the economic potential of the region in the context of national security**. Journal of Advanced Research in Dynamical and Control Systems, 2020, 12(7 Special Issue), c. 1346-1352
39. Alexey Semchenko, Aigul Tulembayeva. **Cataloging of supplies for the armed forces as a mechanism for improving their technical support in the interest of increasing the level of military security**. Journal of Advanced Research in Dynamical and Control Systems, 2020, 12(7 Special Issue), c. 1353-1367.